frontiers | Frontiers in Materials

TYPE Original Research
PUBLISHED 18 December 2023
DOI 10.3389/fmats.2023.1327696

OPEN ACCESS

EDITED BY
Kunal Mondal,
Oak Ridge National Laboratory (DOE), United States

REVIEWED BY
Jue Li,
Chongqing Jiaotong University, China
Arnab Bose,
Boehringer Ingelheim, United States

*CORRESPONDENCE
Yannan Shi,
shiynchn@163.com
Jiawei Zhao,
hbzhaojw@163.com

RECEIVED 25 October 2023
ACCEPTED 28 November 2023
PUBLISHED 18 December 2023

CITATION
Wang HQ, Shi YN, Zhao JW, Wang YY, Liu CY and Wu YY (2023), Environmentally friendly concrete material with early strength and fast hardening using coal as an aggregate: a case for supporting empty roadways.
Front. Mater. 10:1327696.
doi: 10.3389/fmats.2023.1327696

Environmentally friendly concrete material with early strength and fast hardening using coal as an aggregate: a case for supporting empty roadways

Hanqiu Wang[1,2], Yannan Shi[3]*, Jiawei Zhao[4]*, Yiying Wang[3], Chengyong Liu[2] and Yuyi Wu[2]

[1]School of Water Conservancy and Hydroelectric Power, Hebei University of Engineering, Handan, Hebei, China, [2]China Coal Energy Research Institute Co., Ltd., Xian, Shanxi, China, [3]School of Mechanical and Equipment Engineering, Hebei University of Engineering, Handan, Hebei, China, [4]School of Civil Engineering, Hebei University of Engineering, Handan, Hebei, China

In order to facilitate ventilation or transportation, many coal mines usually excavate an empty roadway in the middle of the mining working face. Under the influence of mining pressure, empty roadways are easily damaged, seriously threatening coal mines' safety. Because the traditional support method of the empty roadway has the problems of low efficiency, high cost, and low strength, this paper researches the coal-based concrete support material with better effect. The grading test of coal aggregate was carried out, and it was found that the percentage of small-size aggregate greatly influenced the reduction of aggregate porosity in the stacked state. To solve the problems of the high cost of strengthening support methods such as high water material support in empty roadways, which could be more conducive to recovery and reduce coal quality. The research on empty roadways supports concrete material with coal as aggregate, making the working face recover coal resources safely and efficiently. The optimum gradation test of the total is to enhance the strength of support and solve the problem of low power and difficult cementation of coal. Based on the hydration analysis of cementitious material, the coal-based concrete, mainly composed of low-cost slag, is determined. The cementitious material with simple composition, rapid setting, and fast hardening was found. It is proved that the mechanical properties and molding effect of coal-based concrete support composed of gypsum, GGBFS, and clinkercement are better than those of commercial cement. The structural model of "surrounding rock-empty roadways-coal pillar-support" is established. The calculation method and check basis of empty roadways support resistance N_1 are obtained. The results of industrial application verified that coal-based concrete could effectively protect empty roadways without affecting the productivity of coal mines.

KEYWORDS

empty roadway, support, gradation, GGBFS, coal-based concrete, bearing capacity

1 Introduction

Coal, as one of the fossil fuels, is an essential fuel for humanity at this stage. The strike longwall mining method is one of the main methods for large-scale and efficient mining of coal resources. Its biggest feature is that the advancing length of the working face can generally reach thousands of meters. Although this method can reduce the number of moves in the working face and significantly improve the efficiency of coal mining, the long pushing distance makes it difficult to transport the intermediate materials. In order to solve the transportation and ventilation difficulties caused by the long advancing length of the working face, many coal mines often excavate some empty roadways parallel to or at a certain angle with the open-off cut in the middle of the advancing direction of the working face (Ren, 2000; Bai and Hou, 2005; Yin et al., 2018). When the coal mining face passes through the empty roadway, due to the influence of the advanced abutment pressure of the working face, it is straightforward to produce stress concentration, resulting in abnormal ground pressure appearance, frequent occurrence of "coal cannon," and even inducing dynamic disasters such as Rock burst, which significantly endangers the safety of coal mining production (Li et al., 2018; Zhu et al., 2020). Coal mining enterprises have tried to reduce the mine pressure disasters caused by empty roadways. For example, engineers will strengthen the support or fill the roadway when the working face is mined to the empty roadway (Zhang et al., 2013). In addition, some engineers will choose to adjust the angle of the working face or avoid the empty roadway to rearrange the position of the working face. The above methods have only a limited control effect on mine pressure disaster, and there are problems of low efficiency and complicated processes. With the development of material science, more and more cementitious materials are applied to support roadways. Among them, high-water support materials have high strength (Guo, 2002; Wang, 2020) and can support empty roadways. However, the cost of this material is extremely high, and the quality of coal will be reduced when used in the working face, which hinders coal washing. In addition, the stiffness of the empty roadway support body made of high water material is challenging to cut by shearer, which seriously hinders the mining efficiency of the working face. We are inspired by the goaf-filling technology and gob-side entry-retaining technology (Bai et al., 2004; Song et al., 2010; Liu et al., 2020a; Liu et al., 2020b). Suppose the roadway supporting material in the working face can use coal as aggregate and cooperate with the cementing material with rapid solidification, high strength, and low-cost characteristics to form coal-based concrete supporting material. This can ensure the safety of the working face through the empty roadway and recover the coal in the supporting material. This idea can be used as a new method to solve the problem of working faces passing through empty roadways.

Coal is a rock with low hardness, so using coal as an aggregate for concrete will face the drawback of low strength. However, on the other hand, due to the low density of coal compared to other rocks, it presents loose and porous characteristics, which is favorable to increase the contact area between the coal pieces and the powdered cementitious material. However, the particles of the cementitious material must be small enough. The metallurgy and coal-fired power plant industries related to coal mines produce a large amount of solid waste that is harmful to the environment, such as slag powder and fly ash. Suppose the solid waste produced by the industry can be used as the primary cementitious material along with the coal produced by the coal mine to make concrete. In that case, it can solve the problem of solid waste emissions and improve the efficiency of coal utilization, which is a two-for-one benefit.

Given the above characteristics, this paper utilizes the characteristics of coal aggregate with many pores to enhance the cohesive force of cementitious materials and thus shorten the setting time of concrete; on this basis, we experimentally investigated the concrete ratio when coal is used as the aggregate. After that, we continued to study the mechanical properties required for coal-based concrete to support the empty roadway and verified the supporting effect of coal-based concrete through industrial tests. This research is of great practical value to ensure the safe production of coal mines and improve the utilization of coal resources and industrial solid waste.

2 Aggregate size grading

The concrete is composed of cementitious materials, aggregates, etc. It has both compression and load-bearing characteristics. Concrete is an excellent support material. The aggregates are an essential factor in determining the mechanical properties of concrete. In concrete systems, aggregates generally use composite grading with multiple particle sizes. In addition, the particle size distribution of aggregates plays a crucial role in the bonding performance of concrete materials. Reasonable aggregate size grading can improve the compactness of materials and is beneficial for the early stability of concrete (Wang et al., 2016).

2.1 Aggregate size grading design

The coal produced by the stope is blocky. When stacked, coal blocks' compactness depends on the particle size distribution. Ungraded coal blocks as aggregates are not conducive to the early stability of the support body. Moreover, when the raw coal is not broken to a specific particle size, it can easily block the pipe when pumped as concrete aggregate. This will significantly reduce the construction efficiency of concrete support. With Pipeline transport as the background, to obtain the optimal grading scheme when coal is used as aggregate, we select aggregate with particle size not exceeding 20 mm (Liu and Zhao, 2010) through screening to carry out porosity tests in the laboratory. Based on the continuity of grading and conventional screening conditions, we divide aggregates smaller than 20 mm into three types according to their particle size, representing small, medium, and large particle

TABLE 1 The size classification of aggregate.

Particle size (mm)	Relative classification
0–5	Small-size
5–10	Medium-size
10–20	Large-size

TABLE 2 The scheme of aggregate grading.

Number	Aggregate size grading (weight fraction)		
	10–20 mm	5–10 mm	0–5 mm
1	0	0	10
2	0	2	8
3	0	4	6
4	1	3	6
5	2	2	6
6	3	1	6
7	4	0	6
8	6	0	4
9	3	3	4
10	1	6	3
11	0	6	4
12	0	8	2
13	4	4	2
14	6	4	0
15	8	0	2
16	10	0	0

sizes in order. The particle size classification of aggregates is shown in Table 1.

Small-size aggregates can fill the voids in concrete. However, when the proportion of small particle size aggregates is too high, it will prolong the self-stable molding time of the concrete body and is not conducive to increasing its strength. Therefore, based on the mass fraction of small-size aggregates, the proportion of small-size aggregates decreased from 10 to 0, and 16 groups of size gradation were designed. Each group of schemes is shown in Table 2.

2.2 Aggregate grading characteristics test

Some articles often use the compressive strength or compressibility method to determine aggregates' stacking characteristics in the analysis of aggregate grading experiments (Qie et al., 2021). First, the aggregate is loaded into a high-strength mold. Then, different pressures are vertically applied using a hydraulic press to test the strain of the aggregate in the stacked state. The mechanical properties of the aggregate limit this experimental method - when the loading pressure is too high, it can cause the aggregate to break down into smaller particles. It will change the designed aggregate grading and result in interference with the results. When the loading pressure is too low, not enough compression rate data will be measured in the experiment. The compactness of aggregate accumulation cannot be accurately reflected. When coal is used as aggregate, it is more likely to break under pressure, and the above situation occurs. Therefore, we need to change the method to ensure that the shape of coal aggregate particles does not change during the experimental process. This can improve the accuracy of the experiment.

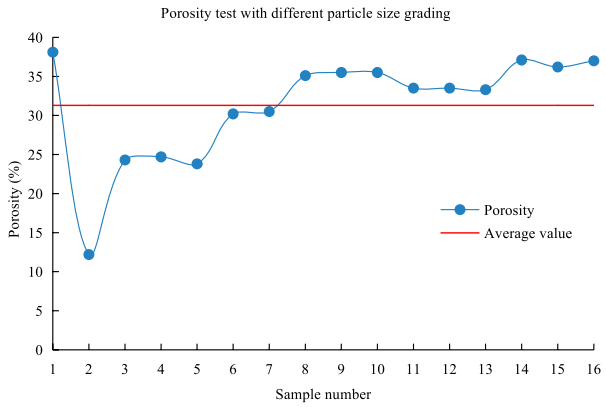

FIGURE 1
The porosity curve of different particle size grading.

The newly designed test scheme draws lessons from Archimedes' principle - water is used as a medium, and a large measuring cup is used as a container. When we add a certain amount of water to the aggregate in the stacked state, the gaps between the aggregate particles are filled with water, which will cause the level in the measuring cup to drop. We can obtain the porosity of the aggregate in a stacked state by measuring the ratio of the volume of the falling part to the overall volume of the aggregate. The principle is to calculate the volume of pores between aggregates in a stacked state to determine the optimal aggregate grading.

The larger the container, the more it can avoid the adverse impact of the randomness of aggregate accumulation on the results. Therefore, we use a 5,000 mL acrylic measuring cup. The diameter of this measuring cup is 130 mm, and the height is 160 mm. The calibrated error of this measuring cup is about ±70 mL, with an error rate of 1.4%. The error of the measuring cup is within a reasonable range. The screened coal aggregate was soaked in water for 48 h before the experiment. The purpose of doing so is to prevent the aggregate from absorbing water and causing interference with the test results. After the aggregate is soaked, it is wiped dry and tested according to the grading scheme in Table 1. The average weight of coal blocks below 20 mm per 2000 mL in a stacked state is approximately 2,700 g. Therefore, the samples for each plan are prepared with a total mass of 2,700 g, and coal aggregates with different particle sizes are weighed according to their respective weight fractions.

Experimental steps: Firstly, the samples of each grading scheme are loaded into 5,000 mL measuring cups. Secondly, the aggregate in the measuring cup is shaken by the ZS-15 vibration device for 30 s to reduce the randomness of aggregate accumulation. Thirdly, the aggregate volume is read from the four sides of the measuring cup, and the average value is taken for recording. Finally, the measuring cup containing aggregates is poured into 2000 mL of clean water, and the liquid level is observed. We tested each scheme three times and took the average value to obtain the porosity curves of different schemes.

2.3 Porosity characteristics of coal as aggregate in a stacked state

The aggregate as a whole can be regarded as a Porous medium material. As is well known, the smaller the pore space in the aggregate in a stacked state, the denser it becomes. φ it represents the porosity of aggregates in the packing state measured experimentally. The formula for calculating porosity is:

$$\varphi = \frac{V_W + V_S - V_L}{V_S} \times 100\% \quad (1)$$

Where φ is the porosity, %; V_W is the volume of water, 2000 mL was taken for this experiment; V_S is the total volume of aggregates in a saturated state, mL; V_L is the liquid level volume reading after pouring water into the aggregate, mL.

The porosity of 16 groups of particle-size grading samples measured in the experiment is shown in Figure 1.

From the test results, it can be intuitively observed that when the aggregate is a single particle size - all large or small- or without small particle size composition, the porosity is over 37%. The skeleton network formed by uniform particles lacks an effective fill of small particles, which is not conducive to the dense accumulation of concrete. We compared samples 3, 4, and 5 with samples 6, 7, 8, and 9 and found that when the proportion of small particle size aggregates is fixed, the porosity of aggregates in the stacked state tends to be consistent, with a difference of less than 1%. At this time, the overall porosity is slightly lower when the content of aggregates in other particle size ranges, except for small particle size aggregates, is more uniform, such as samples 5 and 9, but the impact is insignificant. We also compared and analyzed samples 2-7 and found that under the condition where the content of small particle size aggregates is the majority-mass ratio>50% - the overall porosity of the aggregates is lower than the average level. At this time, the larger the content of larger particles in other particle size aggregates except for small particle size aggregates, the higher the porosity. For example, the porosity of samples 6 and 7 is greater than that of samples 3, 4, and 5, while the porosity of sample 2 is less than that of samples 3, 4, and 5. These findings are consistent with many aggregate grading papers - the proportion of small particle size aggregates significantly impacts the stacking effect. It is easy to find that the porosity of the No. 2 grading sample is significantly better than that of other samples. Overall, when the weight ratio of different particle sizes to small particle sizes is 2–4:6-8, and the porosity of the aggregate in the stacked state is lower and more dense.

When aggregates are stacked, it is mainly larger-sized aggregates that form the skeleton of the entire material. In contrast, smaller-sized aggregates fill the pores between the frames, significantly reducing the pore space of the aggregate support material. Aggregates of different sizes are squeezed and connected to form a skeleton grading network. Therefore, the proportion of small particle-size aggregates significantly impacts the pore space of the aggregates (Tu et al., 2009). When these conclusions are used in industrial production, it is often impossible to divide aggregates into multiple particle size ranges due to the large production capacity of crushing and screening equipment. Based on the analysis above and equipment research, in practical application, it is only necessary to statistically analyze the distribution characteristics of the discharge particle size of the crushing equipment and control the yield of fine particles through corresponding adjustment devices to make the particle grading of the aggregate more reasonable and achieve an optimal grading scheme. For example, a jaw crusher can adjust the tension spring and adjustment block behind the crusher. The impact crusher controls the discharge particle size distribution by adjusting the clearance between the castor bars below the machine. The roller crusher changes the particle size distribution through a wedge-shaped or gasket adjustment device installed between two roller wheels, and general crushing equipment can achieve control of satisfactory particle yield.

3 Cementitious material for concrete using coal as aggregate

3.1 The hydration reaction mechanism of cementitious materials

There are two main differences between the mining concrete system and the surface: The working space is narrow, and the concrete curing time is short. On the other hand, the temperature and humidity inside the roadways are relatively constant, which is beneficial for applying concrete materials. Based on the above technical features, we have developed a concrete system with raw coal (coal or gangue) as the aggregate for the working face, which can significantly reduce the cost of use. Concrete support materials must have the characteristics of early strength and rapid hardening when applied downhole. However, the strength of raw coal is much lower than ordinary aggregate. Due to its composition and fineness, coal is not easily bonded by ordinary cement. Coal blocks are prone to water absorption, have many surface attachments, and have poor mechanical properties, resulting in low interfacial bonding strength between coal blocks and ordinary cement. When subjected to external forces, slip failure occurs at the bonding interface. When using ordinary cement as a cementitious material in the raw coal aggregate concrete system, there are often defects such as low early strength and long demolding time (Liang, 2015). If special cement is used in coal mines, it is not only expensive but cannot be widely used as a conventional material as we have also found through experiments that the test blocks of special cement cannot be formed in a short period (<30 min), as shown in Figure 4. The common hydraulic cementitious materials are mainly silicate, sulphoaluminate, etc. Although Ground Granulated Blast Furnace Slag (GGBFS) is an impurity generated in metallurgy, it has Volcanic ash activity, which can significantly reduce the material cost when used in cement products. Meanwhile, using this material with volcanic ash properties in cement can significantly reduce the heat released from hydration. The reactivity of GGBFS is significantly enhanced after being stimulated in a specific way, which is very beneficial for the early hardening of cement products and is an ideal adhesive material for coal mining.

GGBFS mainly contains CaO, SiO_2, Al_2O_3, Fe_2O_3, and other components. As a Volcanic ash material, it can be activated in a moderate alkaline environment and continuously react to generate hydraulic Ettringite (AFt). The silica tetrahedron and Ca-O Chemical bond in GGBFS can be depolymerized by OH^- a Chemical bond to form SiO_3^{2-} and Ca^{2+}ions, which can then combine to form C-S-H gel (Li et al., 2016). When GGBFS is used as the main component of cementitious materials, its dosage should be determined while ensuring the bonding ability, which can control the material cost and early strength of the test block.

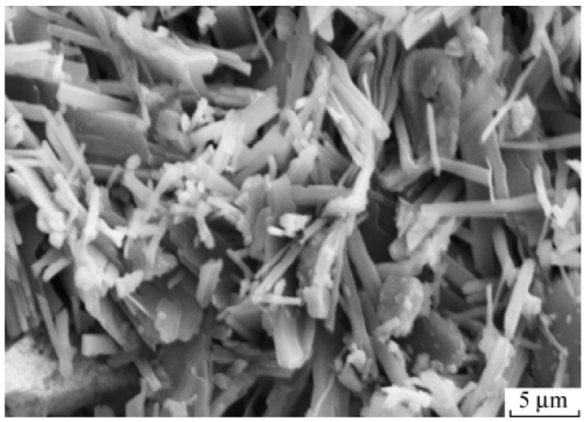

FIGURE 2
Samples in non-alkaline environment.

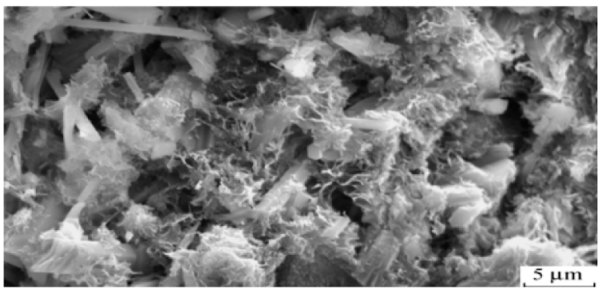

FIGURE 3
Sample in an alkaline environment.

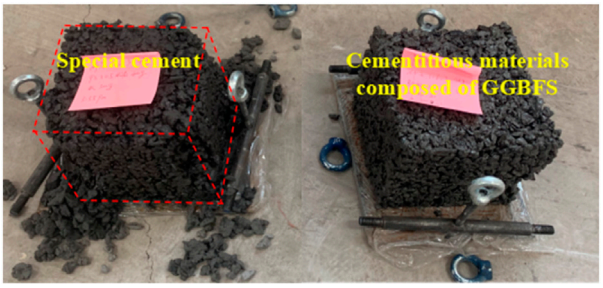

FIGURE 4
Condition of test blocks with different cementitious materials after 30 min.

FIGURE 5
Uniaxial pressure.

Clinker has hydraulicity and is widely studied and applied, making it very convenient to develop a bonding system suitable for coal-based concrete. The cementitious material formed after the clinker activates the GGBFS usually has good long-term cementation performance. The strong alkali Calcium hydroxide directly produced by its hydration reaction can provide an excellent alkaline environment for the slag powder. However, defects such as slow hydration reaction speed and low strength remain. LERCH W discovered as early as 1946 that gypsum has a more prominent performance in improving cement hardening than its retarding effect. Adding gypsum can increase the cement strength by 20%–50% when the SO3 content in the cement is between 3% and 4% (Lerch, 1946). Later, many scholars further confirmed through experiments the promoting effect of gypsum on the cementation performance of clinker-activated GGBFS (Wu et al., 2016).

Gypsum can increase the formation of Ettringite (AFt) and $Ca(OH)_2$ at the initial reaction stage with water, thus improving the strength of the material and avoiding the low early strength of hydration products of GGBFS. In addition, under the dual excitation of gypsum and clinker, the activity of GGBFS is higher than the hydration reaction rate of clinker-GGBFS cementitious material (Qiu et al., 2013). The research on the effect of gypsum on clinker-GGBFS cementitious materials shows that adding an appropriate amount of gypsum can effectively improve the strength of cementitious filling materials (Li et al., 2020).

The curing mechanism of cementitious material mainly composed of GGBFS is that it reacts with water under the double excitation of clinker and gypsum to generate C-S-H gel and Ettringite (AFt). The general reaction process is as follows (Zhang, 2016; Li et al., 2020):

C-S-H gel at room temperature:

$3CaO{\cdot}SiO_2+nH_2O \rightarrow xCaO{\cdot}SiO_2{\cdot}yH_2O+(3-x)Ca(OH)_2$

Ettringite (AFt):

$$Al_2O_3+3Ca(OH)_2+3(CaSO4\cdot 2H_2O)+23H_2O \rightarrow 3CaO\cdot Al_2O_3{\cdot}3CaSO_4{\cdot}32H_2O$$

FIGURE 6
Concrete mold.

Based on the above analysis, the study of concrete with a large amount of GGBFS, an appropriate amount of clinker, and a small amount of gypsum as cementitious materials has great application value in the support direction of coal mines.

3.2 Microscopic morphology of hydration reaction of cementitious materials mainly composed of GGBFS

The microstructure of GGBFS is mostly fine particles, which easily stimulate its potential activity in alkaline environments. The hydration reaction process has improved its microstructure with the participation of alkaline substances such as gypsum clinker. This process was captured by SEM, as shown (Li et al., 2008) in Figure 2 and Figure 3.

It can be seen from Figure 2 that there are still a large number of massive GGBFS that do not participate in the hydration reaction under the non-alkaline environment, and needle-shaped Ettringite (AFt) and spherical C-S-H gel are rarely distributed, preventing the strength and cohesiveness of the sample from further increasing. However, in Figure 3, the particles of GGBFS are not dispersed in an alkaline environment. After the hydration reaction, its particles have been bound and wrapped by reticular C-S-H gel, significantly reducing the void and making the structure more stable. These two figures intuitively confirm significant benefits to the performance of GGBFS-based cementitious materials in alkaline environments.

3.3 Experiment on the mix ratio of clinker-gypsum-GGBFS

Based on the analysis of the hydration reaction process of GGBFS and considering the availability of materials, the optimal components of GGBFS and clinker in cementitious materials are explored through experiments to obtain cementitious materials suitable for use in coal aggregates.

When too much gypsum is added to the cementitious material, it will have a significant retarding effect and hinder the efficient production of the coal mining face. Based on engineering experience, the amount of gypsum we set accounts for 5% of the weight of the cementitious material. Then, the experiment takes the weight of the clinker as a variable to explore the effect of the amount of silicate clinker on the performance of cementitious materials. When the amount of cementitious material is small, its impact on the shaping effect of the concrete system can be fully verified. The weight ratio of cementitious material to aggregate designed in this section is 1:10. The aggregate grading is based on the No. 2 sample in Section 2.3. The above materials are mixed and loaded into the mold, compacted, and left to stand for 30 min before demolding. Test blocks that can be molded quickly indicate that the cementitious material is well bonded to the coal. The amount of water used for mixing is 0.5 times the weight of the cementitious material. After demolding, we checked the condition of the test blocks and then put them into the curing box for 7 days and 28 days, respectively, and three test blocks were made for each group. Due to the high humidity and constant temperature in the underground coal mine, the curing condition of concrete was set at 25°C and 92% humidity. Finally, we utilized a uniaxial press to conduct compressive tests on the blocks at the end of the curing, and the results of each group of test blocks were averaged. The test results are shown in Table 3.

From the experimental results, it can be seen that when the content of silicate clinker is 25%, the strength of the earlier test blocks reaches the best, followed by 10% of silicate clinker content. The 7-day strength of both a_1 and a_4 test blocks exceeded 3 MPa. From the experimental results, controlling the amount of clinker can help accelerate the early hydration reaction rate of the test block to a certain extent (Bazaldúa-Medellín et al., 2015) (As shown in test block a_1). As the amount of clinker increases, sufficient calcium silicate crystals are provided for the concrete, resulting in a significant increase in the strength of the test block in the later stage. However, this phenomenon is not apparent in the early stages of the hydration reaction (As shown in test blocks a_2 and a_3).

From the perspective of shaping effect, the main component in clinker gypsum GGBFS is S105 grade, which has more excellent activity and fineness. Under the joint excitation of clinker and gypsum, GGBFS, as the main component, not only significantly reduces the material cost but also improves the early bonding ability of the test block, ensuring that the test block is shaped in a short time (30 min). As shown in Figure 4. The left test block in the figure is special cement. On the right is the cementitious material of clinker-gypsum-GGBFS as the test block. We can intuitively see that under the same conditions, the shaping effect of the clinker-gypsum-GGBFS cementitious material is significantly better than that of special cement. The above results are due to the distribution range of crack size in coal ranging from a few millimeters to a few nanometers. The specific surface area of S105 grade GGBFS exceeds 500 m^2/kg, and the particle size is less than 38 μm. The specific surface area of cement is usually between 300 and 350 m^2/kg, and the particle size is less than 80 μm. Therefore, fine-grained GGBFS can better adhere to the pores of coal blocks and improve their binding ability as aggregates. On the other hand, using pozzolanic materials reduces the amount of cement clinker and thus significantly reduces the hydration heat release. Moreover, the total amount of calcium silicate gel is more than that of special cement, so the cementation of the materials is enhanced. In addition,

TABLE 3 Comparative experiment on the dosage of silicate clinker.

Number	Weight fraction (%)	Compressive strength (MPa)	
	Clinker:gypsum:GGBFS	7 days	28 days
a_1	10:5:85	3.23	4.23
a_2	15:5:80	2.22	3.70
a_3	20:5:75	2.28	4.40
a_4	25:5:70	3.48	5.11

if insufficient water is encountered during cement hydration, $Ca(OH)_2$ will be subjected to the action of CO_2 to generate $CaCO_3$, which will lead to the decomposition of the hydrate and destroy its microstructure. This is one of the reasons why test blocks made of special cement cannot be demolded in a short time without maintenance.

Based on the above experimental results, two optimal quality ratios of cementitious materials are obtained, namely: (1) 25% silicate clinker, 70% GGBFS content, and 5% gypsum content; (2) 10% silicate clinker, 85% GGBFS content, and 5% gypsum content.

4 Experimental study on mechanical properties of coal aggregate concrete

4.1 Design of experimental plan

The strength of concrete with coal aggregate must be verified when used as a coal mine support material. We conduct compressive strength tests with the help of uniaxial press and concrete mold. To ensure that the coal aggregate concrete is easy for the shearer to recover effectively, the coal content in the concrete should be at least 60%. The recycling process of coal-based concrete is as follows: when the coal mining face advances to the empty roadway, the shearer directly cuts the coal-based concrete in the empty roadway because the coal aggregate is easily cut. The cut coal-based concrete falls into the scraper conveyor below the shearer and then is transferred to the belt conveyor, leaving the coal mining face and being transported to the coal preparation plant. After the broken coal-based concrete reaches the coal preparation plant, the coal resources will be sorted through jigging or dense medium selection methods. The higher the coal content, the more favorable it is for the coal mine to recover its resources. In actual experiments, the weight of coal accounts for 65% of the solid material, which can effectively ensure coal recovery. Aggregates and cementitious materials directly influence the strength of concrete support. We tested concrete's shaping time and material strength with a 65% coal content.

The experimental aggregate grading is Scheme 2 in Section 2.3. We use Portland cement (P.O 4.25) and Sulfoaluminate cement (R.SCA 42.5) as comparative cementitious materials. The dosage of clinker, gypsum, and GGBFS is selected according to Table 3, where a_1 corresponds to the A1 test block, a_2 to the A2 test block, a_3 to the A3 test block and a_4 to the A4 test block. Three test blocks were made for each scheme. The equipment used in the experiments consisted of a YA-300 uniaxial press and 150 mm^3 molds. Among them, the YA-300 uniaxial press can apply a force of up to 300 kN. After the concrete is mixed and compacted, let it stand at room temperature for 30 min to demolding, then perform maintenance. Due to the high humidity and constant temperature in the coal mine underground, the curing conditions for concrete are set at 25 °C and a humidity of 92%. The experimental setups are shown in Figures 5–7.

FIGURE 7
Concrete curing box.

4.2 Test results of coal aggregate concrete

We analyzed the demoulding time, and compressive strength from 1 to 28 days of test blocks with different cementitious materials. The record of the experiment is shown in Figure 8. As a whole, coal-based concrete test blocks made of Portland cement and sulfoaluminate cement their strength growth is a gentle process, indicating that the solidification of coal aggregate by such cementitious materials is slow and progressive; in contrast to coal-based concrete test blocks made of clinker, gypsum, and GGBFS, there is a significant process of growth in their strength with the growth of time.

We compared the 1-day strengths of the test blocks. We found that the 1-day compressive strength of coal aggregate concrete test blocks made with clinker, gypsum, and GGBFS was significantly better than that of Portland cement and sulfoaluminate cement. The early mechanical properties of the test blocks were directly

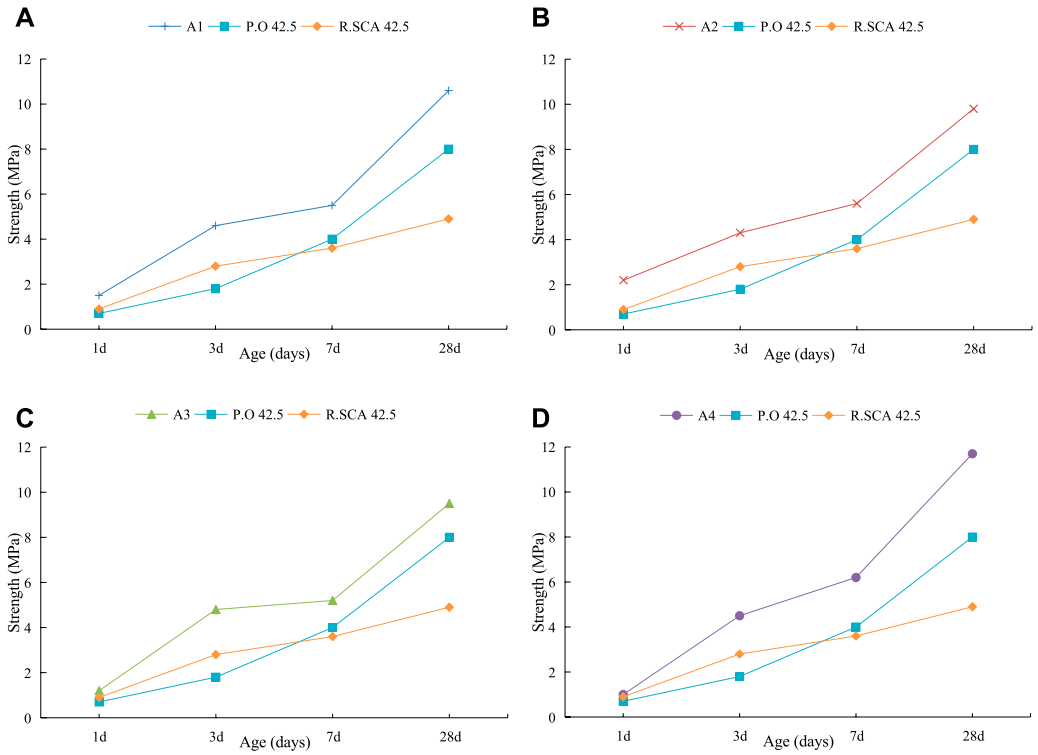

FIGURE 8
The compressive strength of test blocks with different cementitious materials at different ages. **(A)** The comparison of the strength of A1 test blocks with P.O 42.5 test blocks and R.SCA 42.5 test blocks. **(B)** The comparison of the strength of A2 test blocks with P.O 42.5 test blocks and R.SCA 42.5 test blocks. **(C)** The comparison of the strength of A3 test blocks with P.O 42.5 test blocks and R.SCA 42.5 test blocks. **(D)** The comparison of the strength of A4 test blocks with P.O 42.5 test blocks and R.SCA 42.5 test blocks.

correlated with the cementitious materials' ability to coagulate. This demonstrated that the early adhesive properties of clinker, gypsum, and GGBFS, a composite, were significantly better than those of cement.

Specifically, the average uniaxial compressive strength of the A4 test block at 28 days was the highest, which was 11.7 MPa, followed by the A1 test block at 10.6 MPa, and the average uniaxial compressive strengths of the A2 and A3 test blocks at 28 days were 9.8 MPa and 9.5 MPa, respectively; the average strength of the coal-based concrete test blocks made of Portland cement at 28 days was 8 MPa, and the lowest average strength of test blocks made of alumina sulfate cement at 28 days was only 4.9 MPa. The average strength at 28 days of the test blocks made with alumina sulfate cement was the lowest, only 4.9 MPa. The above comparison makes it easy to find that the strength at 28 days of the clinker, gypsum, and GGBFS composites increased by 18.75%–46.25% compared with the strength of the test blocks of coal-based concrete made with Portland cement. Moreover, A1 and A4 test blocks have the highest strength.

From a cost perspective, the cost of A1 and A4 test blocks is reduced by 15%–30% compared to concrete test blocks made of cement. From the results of mechanical testing, it can be seen that under the same dosage, grading, and curing conditions, the early strength of concrete test blocks made of clinker, gypsum, and GGBFS composites is relatively high, and an average uniaxial compressive strength of over 10 MPa at 28 days, which can meet the strength requirements of empty roadway support. From the perspective of the shaping effect, the shaping time of concrete test blocks made of Portland cement needs at least 1 h to demoulding. In contrast, the main component of the cementitious material used in the A1 and A4 test blocks is S105 grade GGBFS, which has a specific surface area of not less than 500 m^2/kg and is more active. As the main component (The weight proportion is not less than 70%), it not only significantly reduces the cost of the cementitious material but also improves the solidification ability of the test block, which can shorten the early hardening time. For industrial applications, we chose the formula with the highest compressive strength, the A1 test block, which has a peak compressive strength of 11.7 MPa, to produce the support material.

5 Stability analysis of support structure in the empty roadway

When the support body is applied in the roadway, it is necessary to consider whether its support capacity meets the bearing requirements. During the mining process of the working face, the main roof often exhibits periodic fractures. According to the structural analysis of the "voussoir beam," the B block that is rotating and sinking at a specific moment when the overlying rock structure collapses plays a vital role in the balance of

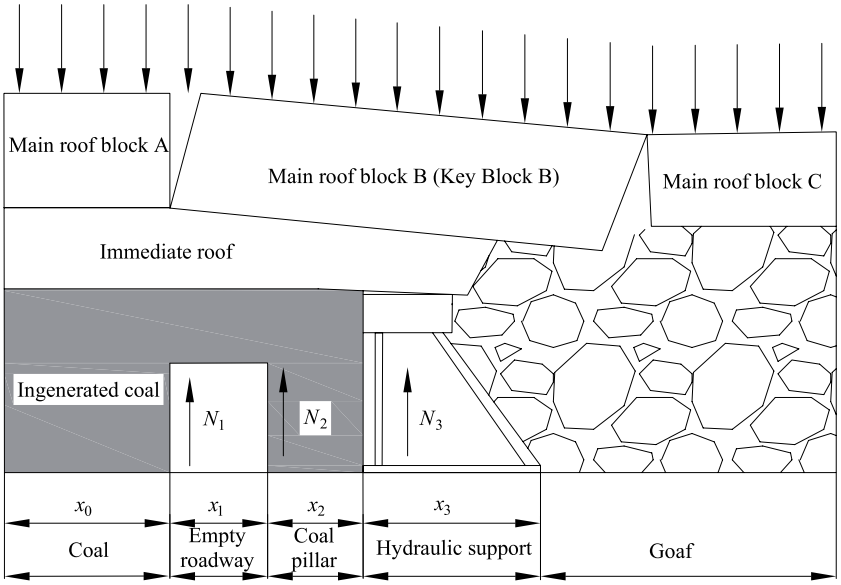

FIGURE 9
The overburden rock structure of an empty roadway.

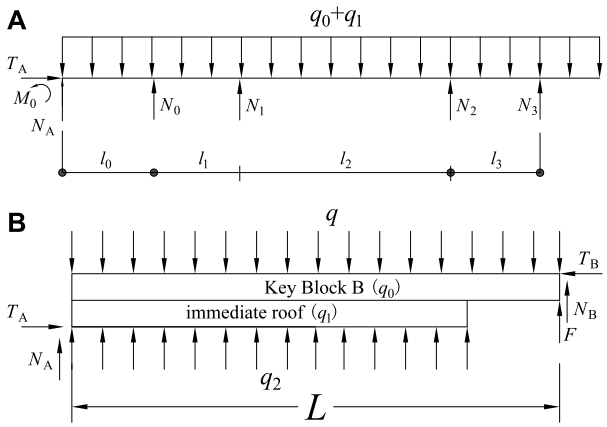

FIGURE 10
The mechanical model of an empty roadway. **(A)** The simplified model of the force state of an empty roadway. **(B)** The force state model of Key Block B and immediate roof.

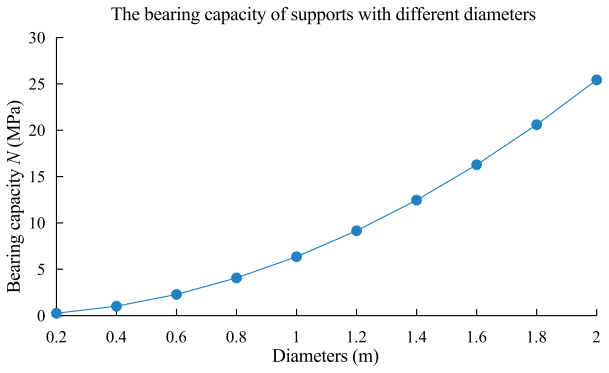

FIGURE 11
The bearing capacity of supports with different diameters.

the structure (Qian and Xu, 2019). As shown in Figure 9. As the working face advances, key block B rotates and cuts off along the roof of the goaf at a specific moment. At this time, key block B and its overlying load are jointly carried by the empty roadway, coal pillar, and working face support (Huang et al., 2015). However, in this state, the coal pillar is often narrow. In the plastic deformation stage of "compression and cracking," the peak stress of the advanced support pressure is located in the surrounding rock of the empty roadway (Xie et al., 2020). This state is very unfavorable for the support of empty roadways. We establish a simplified mechanical model for the support of empty roadways based on this process for analysis.

A mechanical balance is established for analysis based on the stress state of key block B and the immediate roof. When the resultant force of the structure formed by the "overlying rock, goaf, coal pillar, support" is 0, it can be obtained from Figure 10:

$$\begin{cases} q_1 = q_2 \\ (q_0 + q_1)(x_0 + x_1 + x_2 + x_3) = N_A + N_1 + N_2 + N_3 \\ \dfrac{q_1 + q_0}{2}(x_0 + x_1 + x_2 + x_3)^2 = N_1\left(x_0 + \dfrac{x_1}{2}\right) + \\ N_2\left(x_0 + x_1 + \dfrac{x_2}{2}\right) + N_3\left(x_0 + x_1 + x_2 + \dfrac{x_3}{2}\right) \\ q_2(x_0 + x_1 + x_2 + x_3) + F + N_A + N_B = qL \\ \dfrac{q_2(x_0 + x_1 + x_2 + x_3)^2}{2} + FL + N_B L + T_B \Delta S = \dfrac{qL^2}{2} \end{cases} \tag{2}$$

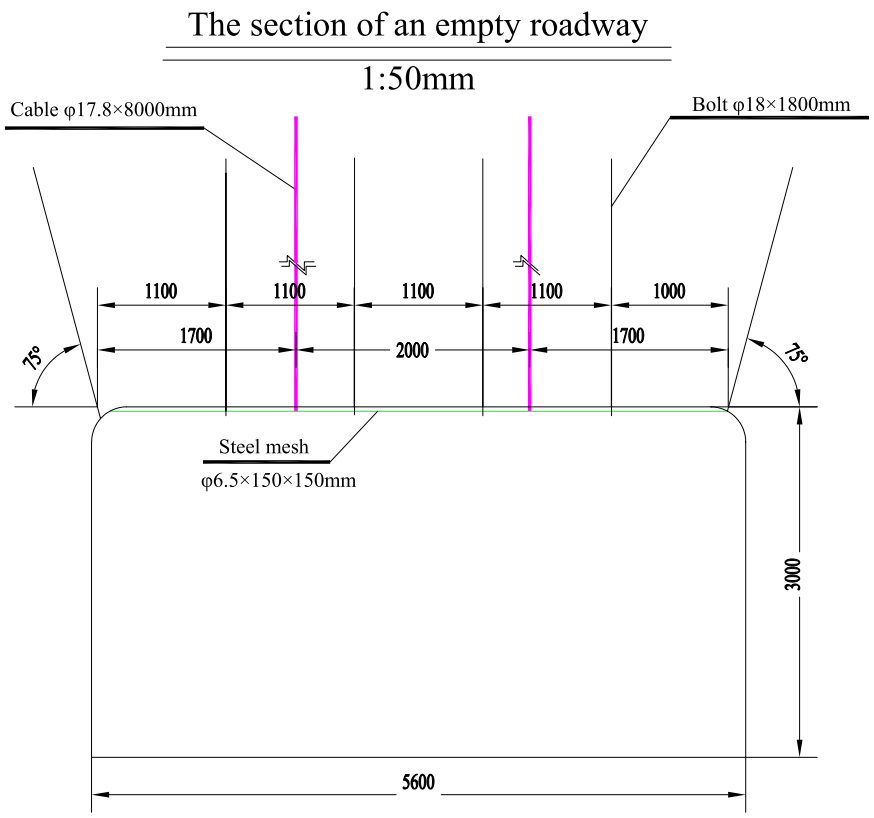

FIGURE 12
The cross-section of an empty roadway.

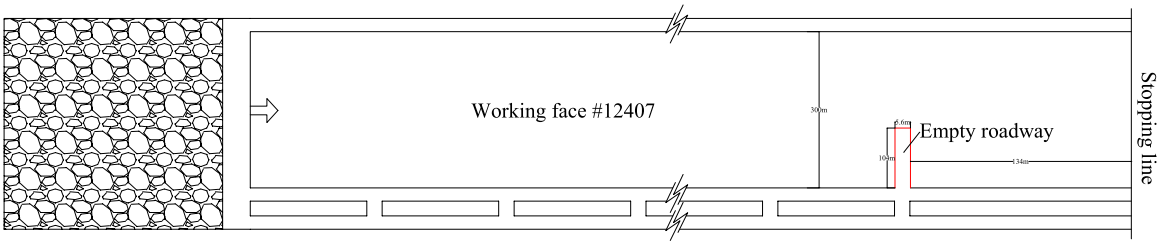

FIGURE 13
Location of empty roadway in working face #12407.

Where x_0 is the practical support range of the coal body, m, which can be taken as 0 based on the most unfavorable principle; x_1 is the width of the roadway section, m; x_2 is the width of the coal pillar, m; x_3 is the support width of the working face support, m; q_0 is the acting force of block B on the immediate roof, kN/m; q_1 is the immediate roof self-weight, kN/m; q_2 is the support force of the structure formed by' empty roadway-coal pillar-support' to the immediate roof, kN/m, $q_2 = q_1$ in the limit equilibrium state; q is the uniform load generated by the weak rock layer above the key block B, which can be taken as the weight of 5–8 times the thickness of B block, kN/m; N_0 is the support force of coal body to roof, kN/m, which can be taken as 0 according to the most unfavorable principle; N_1 is the supporting resistance required for the empty roadway in the equilibrium state, kN/m; N_2 is the supporting force of coal pillar, which can be measured by laboratory mechanical test, kN/m. N_3 is the support resistance of the working face support, kN/m; F is the supporting force formed by roof falling rock, kN/m; N_A is the shear force of rock block A to rock block B, kN/m; N_B is the shear force of rock block C to rock block B, kN/m; L is the length of rock block B, m; $L_2 = h_2R_t/3q$, where R_t is the tensile strength of the main roof. Let $l = x_0+x_1+x_2+x_3$, $l_0 = x_0/2$, $l_1 = x_0+x_1/2$, $l_2 = x_0+x_1+x_2/2$, $l_3 = x_0+x_1+x_2+x_3/2$; T_B is the extrusion force of rock block C to rock block B, kN/m; $T_B = L_2q/2(h\text{-}\Delta S_B)$, where h is the thickness of the main roof B block, m; $\Delta S = h\text{-}\Delta S_B$, ΔS_B is the right-hand subsidence of rock block B when it rotates, m; M_0 is the bending moment of the immediate roof, and 0 is taken in equilibrium.

When solving N_1, according to the mechanical model, it is not difficult to see N_2, N_3, q, q_0, q_1, L, x_1, x_2, and x_3 are known quantities. According to the most unfavorable principle, $x_0 = 0$ can be made. That is, the overburden load is considered to be borne by the structure formed by' empty roadway-coal pillar-support.' The direction of N_B is the same as that of F. When in the limit equilibrium state, it can be made to be $N_B = 0$, and the support resistance required for N_1 empty roadway can be obtained. At this time, there are:

$$N_1 = \frac{\frac{q_1+q_0}{2}l^2 - N_2 l_2 - N_3 l_3}{l_1} \quad (3)$$

The calculation of the bearing capacity of the concrete support body of the empty roadway (China Academy of Building Research, 2015) is as follows:

$$N = 0.9\varphi \times f_c A \quad (4)$$

Where N is the bearing capacity of the support body, MPa or N/mm^2; φ is the stability coefficient of the component, with a maximum value of 1; f_c is the compressive strength of concrete test blocks, N/mm^2; A is the cross-section area, m^2. The bearing capacity of supports with different diameters is shown in Figure 11.

The bearing capacity N of the empty roadway support calculated by Eq. 4 is substituted into Eq. 3 for checking, and the theoretically reasonable design strength of the empty roadway support can be obtained.

$$N \geq N_1 \quad (5)$$

6 Example of coal-based concrete supporting the empty roadway

The fully-mechanized coalface #12407 of the mine is a coal mining face in the #12 coal seam. The floor elevation of the coal seam is 1,180.5–1,199.5 m, and the buried depth of the coal seam is 110–120 m. The working face adopts the inclined long-wall mining method, which is arranged in the east-west direction. The roof and floor lithology of working face #12407 is shown in Table 4. The average coal thickness is 2.4 m. The advancing length of the working face #12407 is 2,450 m, and the width of the working face is 300 m. The stop line is 150 m on the west side of the auxiliary transportation roadway in the fourth panel of the No.12 coal seam. The north of the working face is the unmined working face #12408, the south side is the goaf #12406, and the west side is close to the boundary of the minefield. The empty roadway in the working face #12407 is 134 m away from the west side of the stop line. The size of the empty roadway is 104 m × 5.6 m×3.0 m. The cross-section of the empty roadway is shown in Figure 12. The location of empty roadway in working face #12407 is shown in Figure 13. The working face #12407 was mined to the empty roadway at the end of January 2023.

6.1 Bearing capacity calculation and support scheme of coal-based concrete

When the buried depth of the coal seam is 120 m, the average load q of overlying strata is about 2958 kN/m. L is the measured main roof periodic weighting, and the average distance is 20 m. According to the most unfavorable principle, the working face has been cut to the empty roadway without a coal pillar. At this time, $N_2 = 0$. N_3 is the support length of hydraulic support, which takes 2069 kN. $T_B = L_2 q/2(h\text{-}\Delta S_B)$, h is the thickness of the main roof, and we take the average of 17.8 m. The accumulation height behind the immediate roof's collapse is considered half of the mining height. Currently, the ΔS_B on the side of the goaf of the key block B is 1.2 m. After simple calculation, we can get T_B is 35,638.6 kN/m, ΔS is 16.6 m. The average weight of the main roof is 890 t, and the average load q_0 is about 438.77 kN/m. The average thickness of the immediate roof is 6.6 m, and the q_1 is about 162.69 kN/m. After simple calculation, we can get that l is 11.4 m, l_1 is 2.8 m, l_2 is 5.6 m, l_3 is 8.5 m. Substituting the above parameters into Equation 3, $N_1 \approx$ 7,677.3 kN can be obtained.

According to Formula (4) and taking the uniaxial compressive strength of the A4 test block, the supporting force of coal-based concrete support (pier column) with different diameters is obtained, as shown in Table 5.

We can find from the table that when the diameter of the support is greater than or equal to 1 m, $N > N_1$, which indicates that the coal-based concrete support not less than 1 m can theoretically meet the needs of the support strength of the empty roadway. Therefore, we chose the coal-based concrete support with a diameter of 1 m to support the empty roadway in the industrial test. The height of each support is the same as the height of the empty roadway. In order to compare the supporting effect, we set up single-row supports and double-row pillars in different positions on the empty roadway. The center distance of a single row of supports is 2.5 m, and the support length is 20 m. The double-row supports are arranged on the inner side of the empty roadway, with a spacing of 2.2 m by 2.5 m, and the support length is 40 m. The total support length of the coal-based concrete support in the empty roadway is 60 m, with 39 supports. The scheme of the industrial experiment is shown in Figure 14.

The mold bears the weight of concrete during the pouring process and must ensure a specific strength. Q235 steel is used to make molds to ensure their strength. The thickness of the mold is 2.5 mm, and the inner diameter is 1 m. The mold is made by splicing multiple segments, making it easy to disassemble and adjust in height. Each segment of the mold is linked by metal pins, allowing for quick installation. The mold is shown in Figure 15. A single coal-based concrete support is divided into three sections to set up a mold in the empty roadway, and the height of each pouring is 1 m.

6.2 Analysis of industrial experimental results

The mining progress of the working face: On 27 January 2023, during the morning shift, the working face was 18 m away from the empty roadway. On 28 January, during the morning shift, the working face was 10 m away from the empty roadway. After the end of the middle shift on the same day, the working face was 5 m away from the empty roadway. On 29 January, during the middle shift, the working face was connected to the empty roadway. During the night shift of the same day, the working face smoothly passed

TABLE 4 Roof and floor lithology of working face #12407.

Roof and floor	Lithology	Thickness (m)	Rock character
Main roof	Medium grained sandstone	4.0–31.6	Gray, grayish white, fine-grained structure, massive structure, the main component is composed of quartz, feldspar, etc., with medium-grained sandstone
Immediate roof	Fine-sandstone	3.1–10.1	Gray, silty structure, thick layered structure, flat fracture
False roof	Argillaceous sandstone	0.0–0.62	Dark gray, argillaceous cementation containing plant leaf fossils
Immediate floor	Silty sandstone	1.2–6.5	Gray, fine-grained, thickly layered structure, the main component comprises quartz, feldsparetc.

TABLE 5 The bearing capacity of coal-based concrete support with different diameters.

Diameter (m)	Compressive strength of test block (MPa)	Supporting force (kN)
0.8	11	4,970
1.0		7,772
1.2		11,187

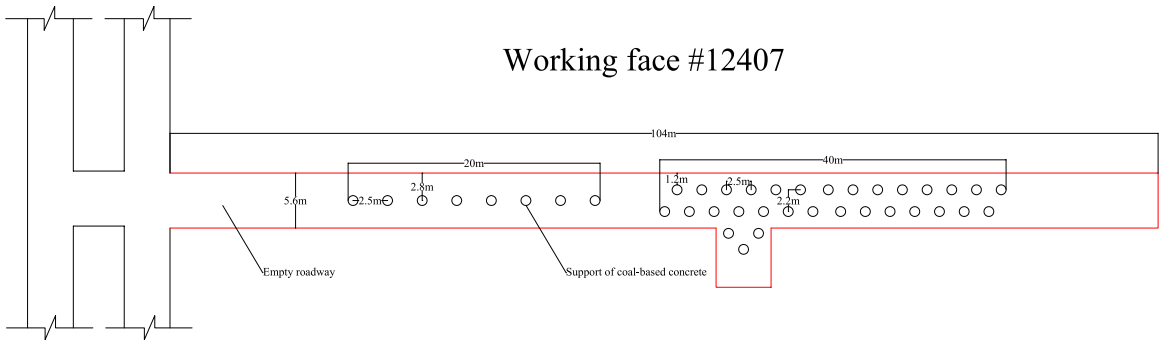

FIGURE 14
Support scheme of empty roadway.

through the empty roadway. In advance, we have set up monitoring instruments for the displacement of the roof and floor in the empty roadway and set up pressure gauges above the coal-based concrete supports to observe the deformation of the empty roadway and the stress on the supports.

The deformation of the space-time roadway 3 m away from the empty roadway in the working face is shown in Figure 16. At this time, eight coal-based concrete supports near the intersection of roadways in the empty roadway showed local cracking, and the remaining 31 supports were intact. The maximum displacement of the empty roadway was observed to be 142 mm. After the working face was connected to the empty roadway, the maximum deformation of the monitored empty roadway was 486.9 mm, located in the center of the chamber in the empty roadway, and the displacement of the top and bottom plates of other monitoring points is less than 200 mm. At the same time, we observed from the working face that the roof of the empty roadway remained intact. When the shearer is mining the empty roadway, the practical stress data of the coal-based concrete supports before they are destroyed are 15.4 MPa and 11.6 MPa, which meets the design requirements of 11.0 MPa. When the shearer is mined, the coal-based concrete supports altogether collapse or topple. The shearer successfully recovered the coal-based concrete supports without any impact on the shearer. The weight of the recovered coal-based concrete is about 156 tons, equivalent to about 2% of the day's coal production, and has no significant impact on the coal quality after coal preparation in the coal preparation plant. The appearance of the roof and coal-based concrete supports of the working face, as well as the corresponding monitoring data, indicate that the coal-based concrete supports can effectively support the empty roadway and ensure the safe mining of the working face. A photograph of the coal-based concrete supports when it is being used industrially is shown in Figure 17.

7 Conclusion

(1) The porosity test of aggregates reveals that the weight ratio of small-size aggregates has an essential influence on aggregates' compacting state when piled up. The optimum aggregate size distribution interval is given as 2–4:6–8 for the weight ratio of

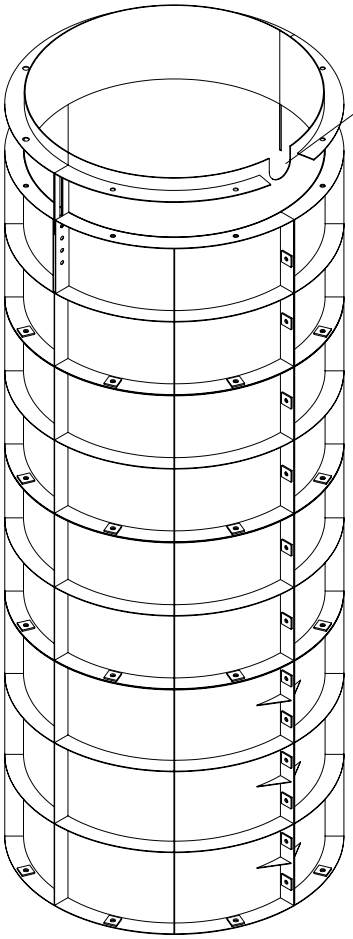

FIGURE 15
Diagram of mold.

small-size aggregate to other sizes, which is simple and easy to obtain and is more suitable for industrial applications than complex continuous grading.

(2) The microscopic analysis of the hydration reaction mechanism and activity characteristics of GGBFS showed that the hydration reaction of GGBFS was more favorable under the double excitation of gypsum and silicate clinker. In addition, GGBFS has finer particles than cement and a lower exothermic amount of hydration, which makes it easier to bond coal. After that, we conducted mechanical tests to investigate the cementing ability of cementitious materials mixed with a large amount of GGBFS (mass fraction more than 70%) and obtained two compositions of cementitious materials that could make the coal aggregate solidify quickly: In one, silicate clinker accounted for 25%, GGBFS accounted for 70%, gypsum accounted for 5%; in the other silicate clinker accounted for 10%, GGBFS accounted for 85%, gypsum accounted for 5%. In the above raw materials, we have respectively utilized the gypsum discharged from coal-fired power plants and the slag powder produced by the metallurgical industry to replace the main ingredient in cement, and this practice improves the utilization rate of industrial by-products and is very beneficial to environmental protection.

(3) We have made coal-based concrete from industrial by-products and coal produced in coal mines, aiming to improve the level of support for empty roadways and utilize coal resources more rationally. We made coal-based concrete test blocks using different cementitious materials with a coal content of about 65% for mechanical testing. The tests showed that the coal-based concrete made from clinker-GGBFS-gypsum composite could be set quickly with uniaxial compressive strength exceeding 10 MPa under the same curing conditions. We found that this cementitious

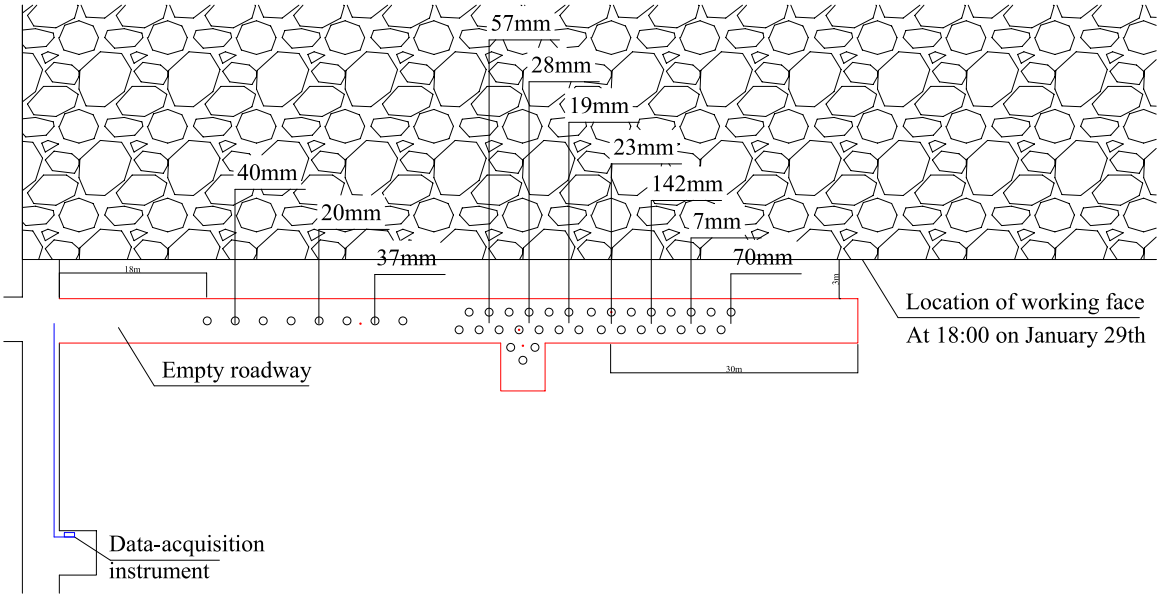

FIGURE 16
The displacement of the top and bottom of the roadway when the working face is 3 m away from the empty roadway.

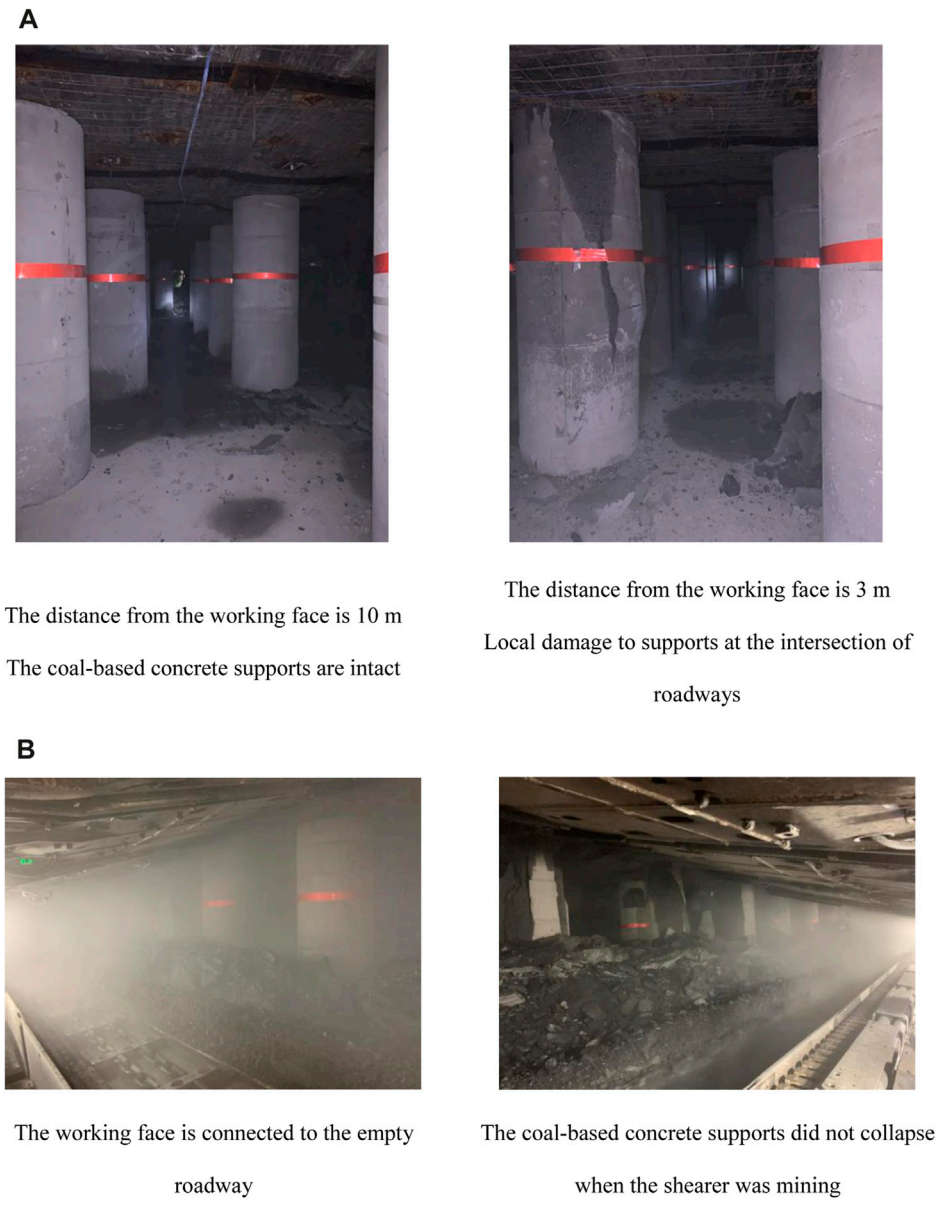

FIGURE 17
Coal-based concrete supports. **(A)** The shearer did not excavate into the empty roadway. **(B)** The shearer excavate into the empty roadway.

material's solidification ability and strength with high GGBFS content when combined with coal are significantly better than ordinary cement or special cement. The advantage of coal-based concrete as the support material of empty roadways is not only reflected in the performance and price. It is more conducive to the shearer cutting coal, improves the production efficiency of coal mining enterprises, and can solve the utilization of industrial by-products. This is a matter which kills two birds with one stone.

(4) We established a mechanical model of an empty roadway. This model is analyzed to obtain the calculation method of the supporting force required for the empty roadway under the influence of overburden movement. We applied this method to design the support scheme of coal-based concrete in the empty roadway, and we made the mold of coal-based concrete. With the help of this model, we can design a more scientific and reliable support program for the empty roadway.

(5) During the working face #12407 passing through the empty roadway, the effective stress before the failure of the coal-based concrete pillar was monitored to be 15.4 MPa and 11.6 MPa, the maximum deformation of the roadway was 486 mm, and the height of the roadway was compressed by about 16.23%, which was mainly affected by the stress superposition at the intersection of the roadway in the empty roadway. The deformation of other positions in the empty roadway is less than 200 mm, and the deformation rate of the roadway is less than 6.7%. During the coal mining process in the working face, the coal-based concrete pillars

did not collapse, which proves that the coal-based concrete pillars we studied can effectively protect the roadway and stop the threat of mine pressure on the empty roadway and the coal mining face.

(6) When the working face is connected with the empty roadway, the roof deformation and pressure near the middle of the working face are higher. If a similar project is carried out, the engineer can design the parameters of coal-based concrete according to the distribution of the hydraulic support force in the working face, combined with the calculation method of the support for the empty roadway proposed in this paper and set double-row columns and single-row columns at different locations in the empty roadway. This method can ensure the effect of empty roadway support and save costs.

Data availability statement

The original contributions presented in the study are included in the article/Supplementary Material, further inquiries can be directed to the corresponding authors.

Author contributions

HW: Writing–original draft. YS: Writing–review and editing. JZ: Writing–review and editing. YiW: Writing–review and editing. CL: Writing–review and editing. YW: Writing–review and editing.

Funding

The author(s) declare financial support was received for the research, authorship, and/or publication of this article. This work was supported by the Central Guiding Local Science and Technology Development Fund Project (Grant number. 236Z1503G); the Hebei Natural Science Foundation Project (Grant number. E2020402064); and the Hebei Innovation Capability Improvement Plan Project (Grant number. 215676140H).

Conflict of interest

Authors HW, CL, and YW were employed by China Coal Energy Research Institute Co., Ltd.

The remaining authors declare that the research was conducted in the absence of any commercial or financial relationships that could be construed as a potential conflict of interest.

Publisher's note

References

Bai, J. B., and Hou, C. J. (2005). Research on principle of roof stability of abandoned workings and supporting technology. *J. China Coal Soc.* 30 (001), 8–11. doi:10.3321/j.issn:0253-9993.2005.01.002

Bai, J. B., Zhou, H. Q., and Hou, C. J. (2004). Development of support technology beside roadway in goaf-side entry retaining for next sublevel. *J. China Univ. Min. Technol.* 33 (2), 183–186. doi:10.3321/j.issn:1000-1964.2004.02.014

Bazaldúa-Medellín, M. E., Fuentes, A. F., and Gorokhovsky, A. (2015). Early and late hydration of supersulphated cements of blast furnace slag with fluorgypsum. *Mater. Construcción* 65, 1–13.

China Academy of Building Research (2015). *Design code for concrete structure GB50010-2010*. China: China Architecture and Building Press.

Guo, J. G. (2002). Technique of filling roof-collapsed roadway with material with high water content in fully-mechanized top-coal caving faces. *J. China Univ. Min. Technol.* 2002 (06), 82–85. doi:10.3321/j.issn:1000-1964.2002.06.020

Huang, W. P., Gao, Y. F., and Wen, Z. J. (2015). Technology of gob-side entry retaining using concrete-filled steel tubular column as roadside supporting. *J. China Univ. Min. Technol.* 44 (4), 8.

Lerch, W. (1946). The influence of gypsum on the hydration and properties of portland cement pastes-discussion. *Proc. Am. Soc. Test. Mater.* 46, 1252–1291.

Li, H., Xing, J., and Zhao, Y. L. (2016). Experiment of new cementing material based on blast furnace slag. *Nonferrous Met.* 68 (6), 4. doi:10.3969/j.issn.1671-4172.2016.06.012

Li, L. T., Gao, Q., and Chen, D. X. (2020). Effect of gypsum–clinker mass ratios on properties of slag filling cementitious material and its application. *J. Central South Univ. Technol.* 51 (2), 10–11817.

Li, L. Y., Shi, Z. L., and Ai, Y. P. (2008). Alkaline activation of gypsum-granulated blast furnace slag cementing materials. *J. Chin. Ceram. Soc.* 36 (3), 405–410. doi:10.3321/j.issn:0454-5648.2008.03.028

Li, S. R., Wang, H. Q., and Wang, Y. L. (2018). Characteristics of accidents with strong mine pressure under influence of coal mining in nariingol no. 2 coal mine. *Coal Eng.* 50 (05), 80–83. doi:10.11799/ce201805020

Liang, Z. Q. (2015). Review on development and application of new type backfilling Cementing materials in mining industry. *Metal. Mine* 2015 (6). doi:10.3969/j.issn.1001-1250.2015.06.035

Liu, J. G., Li, X. W., and He, T. (2020a). Application status and prospect of backfill mining in Chinese coal mines. *J. China Coal Soc.* 45 (1), 141–150.

Liu, J. G., Wang, H. Q., and Zhao, J. W. (2020b). Review and prospect of development of solid backfill technology in coal mine. *Coal Sci. Technol.* 48 (9), 27–38. doi:10.13199/j.cnki.cst.2020.09.003

Liu, J. G., and Zhao, Q. B. (2010). Comprehensive mechanized filling coal mining. *J. China Coal Soc.* 35 (9), 6.

Qian, M. G., and Xu, J. L. (2019). Behaviors of strata movement in coal mining. *J. China Coal Soc.* 44 (04), 5–16.

Qie, L., Shi, Y. N., and Liu, J. G. (2021). Experimental study on grouting diffusion of gangue solid filling bulk materials. *J. Min. Strata Control Eng.* 3 (2), 023011. doi:10.13532/j.jmsce.cn10-1638/td.20201111.001

Qiu, X. R., Wang, L., and Qi, Y. Y. (2013). Study on the mechanism of early hydration of gypsum slag cement. *Cement* 2013 (07), 1–4.

Ren, D. Y. (2000). Discussion on the feasibility of continuous coal mining through goaf in fully mechanized mining face. *Shanxi Coal* 2000 (2), 24–26.

Song, Z. Q., Cui, Z. D., and Xia, H. C. (2010). The fundemental theoretial and engineering research on the green safe no coal pillar mining model by mainly using coal gangue backfill. *J. China Coal Soc.* 035 (005), 705–710. doi:10.1016/S1876-3804(11)60004-9

Tu, Q., Z, X. F., and Liu, P. L. (2009). Experimental study on compression deformation of coal gangue dispersion with different particle size. *Coal Eng.* 2009 (11), 68–70.

Wang, W. (2020). Application of high water material filling pillar in overpass alley of high cutting working face. *Coal Eng.* 52(5), 67–70.

Wang, W., Li, H. M., and Xiong, Z. Q. (2016). Research on the influence of diameter gradation on compressive deformation characteristics of gangues. *Chin. J. Undergr. Space Eng.* 12 (6), 1553–1558.

Wu, P., Liu, X. J., and Wang, J. X. (2016). Effect of anhydrite on hydration of clinker activated slag cementing materials. *J. China Univ. Min. Technol.* 45 (3), 615–622.

Xie, S. R., Pan, H., Chen, D. D., Zeng, J. c., Song, H. z., Cheng, Q., et al. (2020). Stability analysis of integral load-bearing structure of surrounding rock of gob-side entry retention with flexible concrete formwork. *Tunn. Undergr. Space Technol.* 103, 103492. doi:10.1016/j.tust.2020.103492

Yin, C., Feng, G. M., and Gao, P. (2018). Research on instability mechanism of surrounding rock in stage of working face passing abandoned roadway. *J. Min. Saf. Eng.* 035 (003), 457–464. doi:10.13545/j.cnki.jmse.2018.03.002

Zhang, Z. (2016). Experimental study on physicochemical and mechanical properties of composite cementing material for backfill mining. *Coal Eng.* 48 (2), 91–94. doi:10.11799/ce201602028

Zhang, Z. Z., Bai, J. B., and Han, Z. T. (2013). Roof mechanics analysis and backfill technology for abandoned roadway. *J. Min. Saf. Eng.* 030 (002), 194–198.

Zhu, G. G., Jiang, Q. P., and Wu, Y. P. (2020). Reasonable determination of terminal mining line using technology of stress field with seismic wave in deep coalfaces. *J. Min. Saf. Eng.* 45 (S2), 571–580. doi:10.13225/j.cnki.jccs.2020.0508